# Resonant cavity enhanced light harvesting in flexible thin-film organic solar cells

**Nicholas P. Sergeant,[1,†] Bjoern Niesen,[2,3,†] Albert S. Liu,[1] Lee Boman,[4] Chris Stoessel,[4] Paul Heremans,[2,3] Peter Peumans,[2] Barry P. Rand,[2,*] and Shanhui Fan[1]**

[1]*Electrical Engineering Department, Stanford University, Stanford, California 94305, USA*

[2]*IMEC vzw, Leuven B-3001, Belgium*

[3]*Department of Electrical Engineering, Katholieke Universiteit Leuven, Leuven B-3001, Belgium*

[4]*Southwall Technologies Inc., Palo Alto, California 94303, USA*

**Corresponding author: Barry.Rand@imec.be*

Received January 2, 2013; revised March 28, 2013; accepted March 29, 2013;
posted April 1, 2013 (Doc. ID 182568); published April 24, 2013

Dielectric/metal/dielectric (DMD) electrodes have the potential to significantly increase the absorption efficiency and photocurrent in flexible organic solar cells. We demonstrate that this enhancement is attributed to a broadband cavity resonance. Silver-based semitransparent DMD electrodes with sheet resistances below 10 ohm/sq. are fabricated on flexible polyethylene terephthalate (PET) substrates in a high-throughput roll-to-roll sputtering tool. We carefully study the effect of the semitransparent DMD electrode (here composed of $Zn_xSn_yO_z$/Ag/$In_xSn_yO_z$) on the optical device performance of a copper phthalocyanine (CuPc)/fullerene ($C_{60}$) bilayer cell and illustrate that a resonant cavity enhanced light trapping effect dominates the optical behavior of the device. 

*OCIS codes:* (310.7005) Transparent conductive coatings; (310.6845) Thin film devices and applications; (310.6860) Thin films, optical properties; (040.5350) Photovoltaic.
http://dx.doi.org/10.1364/OL.38.001431

Organic solar cells (OSCs) are promising candidates for large-scale deployment of solar energy conversion because they use thin films of photoactive material and can be manufactured using scalable, cost-efficient, roll-to-roll processes [1]. In the vast majority of OSCs, $In_xSn_yO_z$ (ITO) is used as the transparent electrode material of choice due to its excellent optical and electrical properties. A current challenge for OSCs is that optimal combinations of transparency and sheet resistance for ITO are only achieved at elevated processing temperature [2]. Therefore, good quality ITO is incompatible with low-cost plastic substrates. To overcome this first challenge, the insertion of thin metal layers has been suggested to enhance the lateral conduction of electrodes made of lower-quality ITO deposited at lower temperature [3].

A second challenge of many OSCs is the inherent trade-off between achieving complete optical absorption and good carrier transport. A photoactive film thickness of ~200 nm is typically required to absorb all incident photons, but such thick films are often accompanied by too poor charge transport to allow for complete carrier extraction. To address this trade-off, absorption enhancement strategies based on photonic or plasmonic light trapping have been suggested [4,5]. As the thickness of the organic layers is smaller than the wavelength of the absorbed light, interference effects are unavoidable, but can be exploited to maximize absorption in the photoactive layer by making use of optical spacer effects or spectrally selective semitransparent mirrors [6].

Addressing the challenges above, it has been demonstrated that the use of Ag-based semitransparent electrodes results in an equivalent solar cell performance due to optical cavity effects induced by these electrodes, making them attractive ITO replacements [7–11]. Most of this previous work has been done utilizing polymer photoactive layers. Here, we show that such an equivalent performance is also achievable for ultrathin small-molecule solar cells on flexible substrates. Moreover, the optical cavity effects induced by the Ag-based semitransparent electrode are revealed by experiments as well as optical simulations.

The $Zn_xSn_yO_z$/Ag/$In_xSn_yO_z$ (ZAI) transparent electrodes were sputter deposited onto polyethylene terephthalate (PET) substrates in a custom-built roll-to-roll coater. A schematic of the structure is shown in Fig. 1(a). The 20 nm thick bottom $Zn_xSn_yO_z$ (ZTO) layer behaves as a seed layer for Ag nucleation and can be tuned in thickness to optimize the transmission. A 7 nm unpatterned Ag film is deposited on top of ZTO, followed by a 44 nm thick ITO layer. The Ag film behaves as a semitransparent mirror and at the same time enhances the in-plane conductivity, reducing the overall sheet resistance of the electrode relative to pristine ITO. The top ITO layer can be less conductive by virtue of the presence of the Ag layer and can therefore be deposited at room-temperature. The advantage of this ZTO/Ag/ITO composite electrode is its compatibility with high-throughput manufacturing [12]. A 140 nm thick pristine ITO electrode on PET is deposited at the same deposition conditions and serves as a reference electrode.

The spectral transmission of the ZAI electrode is shown in Fig. 2(a) and compared to the pristine ITO

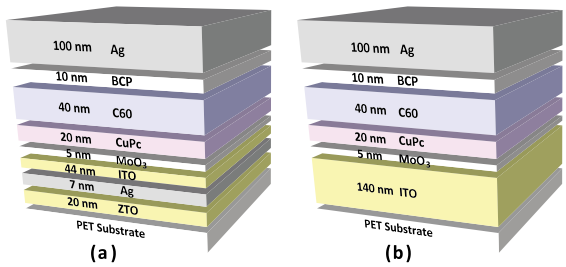


Fig. 1. Device geometry for the solar cells fabricated on the (a) ZAI and (b) ITO anodes.

 

electrode. A good agreement was obtained between the experimental measurements and the optical model using the transfer matrix algorithm. The ZAI electrode and ITO reference have AM1.5G photon density weighted transmissivity ($T_{AM1.5}$) of 77.0% and 78.8%, respectively, in the wavelength range of $\lambda = 400$–$800$ nm. The specular transmission of the ZAI anode exceeds that of the ITO reference in the spectral range of $\lambda = 380$–$610$ nm. Additionally, its sheet resistance measured using a four-point probe is $7.0 \pm 0.5$ ohm/sq., which is significantly lower than that of the ITO reference ($51.7 \pm 0.5$ ohm/sq.). This low sheet resistance can have benefits for large area solar modules, where the series resistance of the solar cell becomes a limiting factor.

Ignoring interference effects, one would expect that, relative to the ITO reference, the total absorption efficiency (TAE) and external quantum efficiency (EQE) of solar cells on the ZAI electrode would be *higher* at $\lambda = 380$–$610$ nm and *lower* at $\lambda > 610$ nm. In contrast, we show here that resonant cavity effects created between the ZAI anode and a reflecting cathode actually lead to an *opposite trend* for thin-film solar cells. To illustrate this effect we have fabricated archetypal copper phthalocyanine (CuPc)/fullerene ($C_{60}$) bilayer solar cells on these electrodes using thermal evaporation. The device geometry is illustrated in Fig. 1 and consists of 5 nm $MoO_3$, 20 nm CuPc, 40 nm $C_{60}$, 10 nm bathocuproine (BCP), and 100 nm Ag, deposited in the same thermal evaporation run on the ZAI anode and on the reference ITO electrode. A shadow mask was used to define an active area of 0.13 $cm^2$.

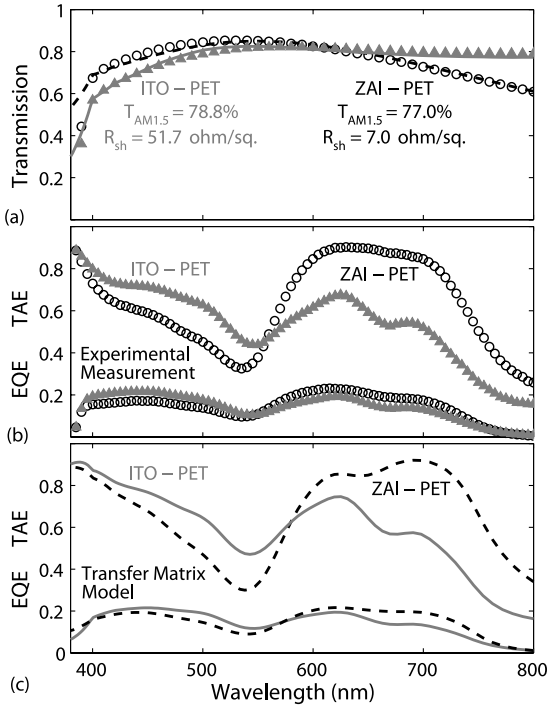


Fig. 2. (a) Measured (markers) and modeled (curves) spectral transmission of the ZTO(20 nm)/Ag(7 nm)/ITO(44 nm) electrode (circles) as well as the reference ITO (140 nm) electrode on PET (triangles). The transmission is referenced to air, and thus includes the reflection and absorption of the substrate. (b) Measured and (c) modeled TAE (top curves) and EQE (bottom curves) for the solar cells on ZAI anode (circles, dashed) and ITO reference (triangles, solid).

In addition to the EQE, the total reflection ($R$) of the solar cells was measured to determine the TAE $= 1 - R$. In Fig. 2(b), the measured EQE (bottom) and TAE (top) spectra are shown for the devices fabricated on top of the ZAI (circles) and ITO anodes (triangles). Even though the far-field transmission of the ZAI electrode without the solar cell stack deposited on it is lower than that of ITO at $\lambda = 550$–$750$ nm [Fig. 2(a)], the TAE of the solar cell on the ZAI anode is significantly higher than that of the ITO reference at this wavelength range, which coincides with the CuPc absorption $Q$-band. The TAE of the solar cell on the ZAI anode reaches values of nearly 90% in the CuPc $Q$-band and even exceeds the far-field transmission, indicative of a resonant cavity that is formed between the ZAI anode and the Ag backreflector/cathode. In contrast, the TAE of the device fabricated on ITO never exceeds the far-field transmission of the bare anode. To understand this trend it is important to note that for the ITO anode, most of the light that is not transmitted is absorbed by the ITO layer. In the bare ZAI electrode, on the other hand, the main loss in far-field transmission is due to reflection, which can be reduced by carefully designing the solar cell structure, leading to a peak TAE beyond what is achievable using ITO electrodes.

To confirm our experimental observation, the measured TAE and EQE are compared to an optical model based on the transfer matrix algorithm combined with an exciton diffusion model [6,8], as shown in Fig. 2(c). The exciton diffusion model assumes 80% charge separation at the donor-acceptor interface and no exciton quenching at the other interfaces. The diffusion lengths of the donor and acceptor were used as fitting parameters and were found to be $L_{D,\mathrm{CuPc}} = 6.9 \pm 0.1$ nm and $L_{D,C60} = 18.0 \pm 0.1$ nm, respectively, in agreement with literature values [13]. An excellent spectral match is obtained between the experimental observation and the optical model for both EQE and TAE.

When optimizing the photon harvesting in a solar cell one needs to maximize the field intensity in its photoactive layer for the desired absorption range. In Fig. 3, the field intensity at normal incidence, $|E_n|^2$, is shown as a function of wavelength and position inside the solar cells on (a) the ITO reference anode and (b) the ZAI anode on PET. The field intensity is normalized to the incoming field intensity. In order to help understand the interference profiles, the position of the first maximum of the field intensity is indicated with a dashed line. In Fig. 3(b), we find that constructive interference of the incoming light between the ZAI anode and the back contact leads to strong enhancement of the field intensity within the CuPc layer in the spectral region of the CuPc $Q$-band. This coherent light trapping effect leads to enhanced absorption and photocurrent for the ZAI anode. In contrast, this resonance effect is not observed for the solar cell fabricated on the ITO anode. It is noteworthy that the maximal optical performance for this thin photoactive layer is obtained when the resonant cavity is tuned to coincide with the CuPc $Q$-band, thus where the absorption is strongest. This is in contrast to many polymer solar cells, which typically exhibit nearly complete

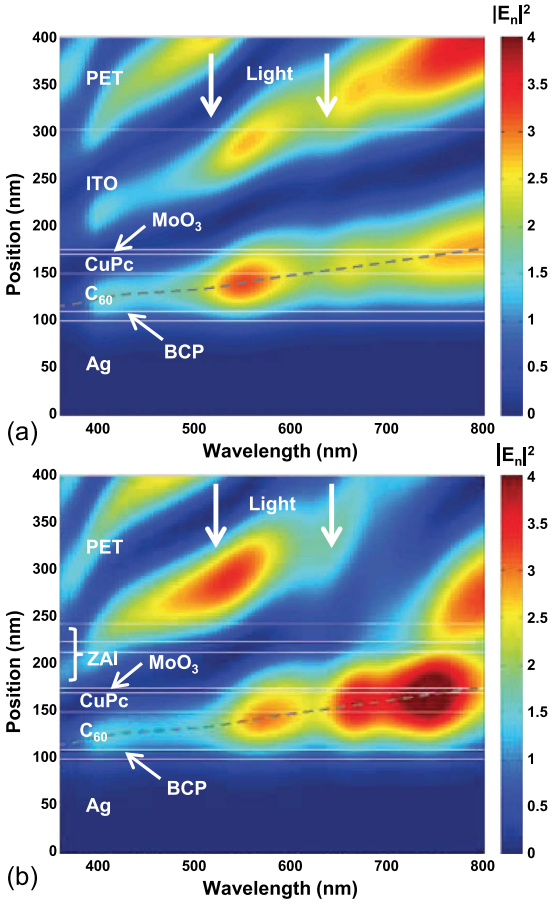


Fig. 3. Normalized field intensity at normal incidence for the solar cells fabricated on (a) ITO and (b) ZAI anodes on PET. Light is incident from the top through the PET substrate. The dashed line approximates the first maximum of the field intensity at $x = \lambda/(4n_{C60})$, where $x$ is the distance from the back contact and $n_{C60}$ is the refractive index of the $C_{60}$ layer.

absorption in their absorption bands, such that only the absorption tails are available for enhancement.

In conclusion, we have fabricated roll-to-roll ZTO/Ag/ITO electrodes with low sheet resistance on flexible substrates. We optimized the optical performance of solar cells on these semitransparent anodes, not by simply maximizing the far-field transmission of the bare electrode, but by tuning the width of the resonant optical cavity formed between the ZAI electrode and a backreflector to maximize the photon harvesting.

This work was partially supported by the Center for Advanced Molecular Photovoltaics (Award No. KUS-C1-015-21), made possible by King Abdullah University of Science and Technology. The authors thank Steve Smout for the patterning of the active device area.

†These authors contributed equally to this work.

## References and Note

1. G. Dennler, M. C. Scharber, and C. J. Brabec, Adv. Mater. **21**, 1323 (2009).
2. V. Sivaji Reddy, K. Das, A. Dhar, and S. K. Ray, Semicond. Sci. Technol. **21**, 1747 (2006).
3. Y.-S. Park, K.-H. Choi, and H.-K. Kim, J. Phys. D **42**, 235109 (2009).
4. S. Basu Mallick, N. P. Sergeant, M. Agrawal, J.-Y. Lee, and P. Peumans, MRS Bull. **36**, 453 (2011).
5. B. Niesen, B. P. Rand, P. Van Dorpe, D. Cheyns, L. Tong, A. Dmitriev, and P. Heremans, Adv. Energy Mater. **3**, 145 (2013).
6. M. Agrawal and P. Peumans, Opt. Express **16**, 5385 (2008).
7. J.-F. Salinas, H.-L. Yip, C.-C. Chueh, C.-Z. Li, J.-L. Maldonado, and A. K.-Y. Jen, Adv. Mater. **24**, 6362 (2012).
8. N. P. Sergeant, A. Hadipour, B. Niesen, D. Cheyns, P. Heremans, P. Peumans, and B. P. Rand, Adv. Mater. **24**, 728 (2012).
9. J. Meiss, M. Furno, S. Pfuetzner, K. Leo, and M. Riede, J. Appl. Phys. **107**, 053117 (2010).
10. W. Cao, Y. Zheng, Z. Li, E. Wrzesniewski, W. T. Hammond, and J. Xue, Org. Electron. **13**, 2221 (2012).
11. W. Yu, L. Shen, F. Meng, Y. Long, S. Ruan, and W. Chen, Sol. Energy Mater. Sol. Cells **100**, 226 (2012).
12. The ZAI electrodes were fabricated on 2 mil thick PET substrates in a dual-drum sputter roll coater with 12″ web width capability and deposition pressure at 6 mTorr. The ZTO layer was sputtered from a ZnSn target of 1:1 ratio at a specific dynamic deposition rate of 107 nm · mm $s^{-1}$ $kW^{-1}$ with an Ar and $O_2$ flow of 20 and 80 sccm, respectively. Silver and ITO were deposited at 50 and 200 nm · mm $s^{-1}$ $kW^{-1}$, respectively. The web coater line speed varied between 5 and 24 mm $s^{-1}$.
13. D. Cheyns, B. P. Rand, and P. Heremans, Appl. Phys. Lett. **97**, 033301 (2010).